

## SCATTERING OF PROTONS IN A THIN GOLD SINGLE CRYSTAL

Yu. N. ZHUKOVA, G. A. IFEROV, A. F. TULINOV, and V. Ya. CHUMANOV

Nuclear Physics Institute, Moscow State University

Submitted February 7, 1972

Zh. Eksp. Teor. Fiz. 63, 217-223 (July, 1972)

Measurements are reported of the scattering of 200- and 500-keV protons in thin single crystals of gold. Angular distributions of the scattered particles were obtained for various angles of incidence of the beam on the target. A qualitative interpretation is given of the dependence of the general pattern of the experimental distributions obtained on the angle of incidence, on the basis of the interaction of ions with individual strings of atoms.

At the present time a considerable amount of experimental data has been accumulated on the interaction of 0.1–10 MeV ions with single crystals whose thickness either exceeds the particle range or is an appreciable fraction of the range. At the same time there are almost no data on the passage and scattering of fast charged particles in single-crystal films of extremely small thickness (100–1000 Å). Use of such thin targets can in principle provide information on the interaction mechanism between ions and individual strings of atoms. Knowledge of this mechanism is extremely important for description of the entire picture of passage of particles through single crystals.

It is well known that an estimate of the average number of collisions of a particle with atomic strings can be obtained by comparison of the thickness  $d$  of the sample with the characteristic length  $\lambda$ , introduced by Lindhard<sup>[1]</sup>, for establishment of statistical equilibrium in the flux of particles moving in the single crystal. Most experiments on channeling and the shadow effect have used targets whose thickness satisfies the relation  $d \gg \lambda$ , which corresponds to a high multiplicity of collisions. In the present work we study some problems of the interaction of particles with crystals whose thickness satisfies the condition  $d \lesssim \lambda$ . In this case the particle experiences a small number of collision events, in particular, single collisions should play an appreciable role.

In order to understand what can be expected from the scattering of particles in such thin films, it is useful to trace qualitatively the interaction process of particles with an individual string. We will introduce a rectangular coordinate system whose Z axis coincides with the axis of the string (Fig. 1). Let a beam of protons parallel to the ZOY plane fall on a string of atoms at an angle  $\theta$ . Two characteristic cases are of interest: 1)  $\theta < \theta_L$  and 2)  $\theta \gg \theta_L$ , where  $\theta_L$  is Lindhard's critical channeling angle.

Since the potential of a string at a small angle of incidence can be considered approximately cylindrically symmetric, for any particle independently of what plane its trajectory lies in, the law of quasimirror reflection is satisfied,  $\theta' \approx \theta$ , where  $\theta'$  is the angle between the particle trajectory after scattering and the string axis. It is evident from this that the trajectories of all scattered particles are grouped near a conical surface with vertex angle  $2\theta$  whose axis coincides with the

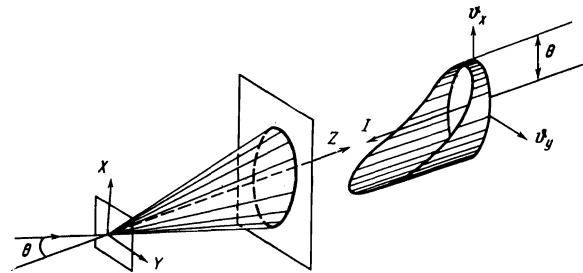


FIG. 1. Schematic drawing of the scattering pattern in a thin polycrystalline target, based on Lindhard's model. The spatial angular distribution of the scattered particles is shown qualitatively in the coordinate system  $\vartheta'_x \vartheta'_y$ .  $I$  is the intensity;  $\vartheta'_x$  and  $\vartheta'_y$  are the respective scattering angles in the planes ZOY and ZOY, measured from the Z axis.

string axis. Consequently, the angular distribution of scattered particles in any section of the cone by a plane passing through the string axis should consist of two peaks, the distance between which is  $\sim 2\theta$ , and the ratio of whose intensities depends on the azimuthal angle of the section. The difference in intensities of the peaks should be maximal in the ZOY plane and should be zero in the perpendicular direction. For an angle relative to the incident beam  $\vartheta_x = 0$  ( $\vartheta_x = \vartheta'_x + \theta$ , see Fig. 1) in the ZOY plane the more intense peak corresponds to almost unscattered particles, and the less intense peak, for  $\vartheta_x \approx 2\theta$ , to particles reflected in quasi-quasimirror fashion. As the angle  $\theta$  is increased from  $\theta < \theta_L$  to  $\theta > \theta_L$  the peaks of the angular distribution are converted into shadow "breastworks" (compensating wings). For  $\theta \gg \theta_L$  the shape of the angular distribution outside the shadow region is already independent of the incident beam direction. Thus, the distance between the peaks in the angular distribution in the region  $\theta < \theta_L$  increases with increasing  $\theta$  and then, beginning at  $\theta \approx \theta_L$ , remains constant, equal to the angular distance between the shadow breastworks  $\theta_b$ .

The region  $\theta \approx \theta_L$  is characterized by the fact that an increase of the angle of incidence is accompanied by an increase in the fraction of protons which penetrate the string. This should lead to an increase in the number of particles scattered into the region outside the reflection cone.

The reasoning presented above applies to scattering of particles by a single string. In view of the finite

thickness of the sample, it is also possible that the interaction of a particle with a single-crystal target does not reduce to a collision with one string, but at the same time complete statistical equilibrium is not yet reached. It is easy to see that in this case the angular distributions of the scattered particles should have much in common with those discussed above. A region of reduced intensity should be observed in the direction of the crystallographic axis. The angular width of this region will increase with increasing  $\theta$ ; here the azimuthal anisotropy of the angular distribution is preserved, although in this case it will not be so sharp as in scattering by a single string. The qualitative features set forth above of the angular distribution of protons scattered in a thin single-crystal film are confirmed by more detailed computer calculations by the Monte Carlo method<sup>[2]</sup>.

In order to study the interaction of protons with atomic strings, we set up experiments in which the scattering of protons in a thin single-crystal of gold was investigated. The targets were prepared by the epitaxial growth method<sup>[3]</sup>; they were used on a collodion backing. The target thickness was chosen so that the relation  $d \leq \lambda$  was satisfied. For protons with energy 500 keV incident on a gold single crystal at an angle  $\theta = \theta_L$  to the  $\langle 100 \rangle$  axis, the value of  $\lambda$  is  $500 \text{ \AA}$ . In our case  $d = 350 \pm 50 \text{ \AA}$ . The area of the gold film was  $9 \text{ mm}^2$ , and the thickness of the substrate  $1000 \text{ \AA}$ . To estimate the degree of perfection of the structure of the thin single crystal we studied the dependence of the yield of particles scattered by an angle of  $30^\circ$  on the angle of incidence  $\theta$  relative to the  $\langle 100 \rangle$  axis (the "reverse" shadow, Fig. 2). The measurements were made for a proton energy  $E = 500 \text{ keV}$ . The shape of the curve in Fig. 2 does not depend on which side of the target was presented to the beam—the substrate or the gold layer, which indicates the small distorting effect of the substrate. If we assume that the finite intensity in the center of the shadow is due mainly to disorientation of blocks with a Gaussian distribution in the disorientation angle, the dispersion of this distribution can be determined on the basis of a simple model (see Ref. 4) describing the change in the shape of the shadow under the action of random deviations of the atomic string axis from its equilibrium position. For  $\delta = Y_1/Y_2 = 0.2$  (see Fig. 2) this model gives for the dispersion a value  $\sigma = 1.5 \pm 0.2^\circ$ . This agrees with the value  $1.5 \pm 0.5^\circ$  obtained by an electronographic method.

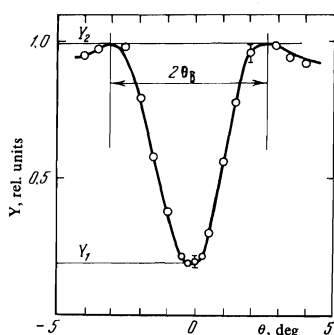


FIG. 2. Yield  $Y$  of protons scattered by  $30^\circ$  as a function of angle of incidence  $\theta$ .

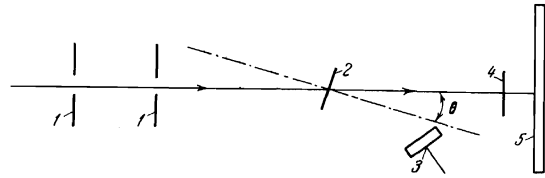


FIG. 3. Experimental arrangement: 1—collimator, 2—target, 3—monitor counter, 4—movable screen, 5—photographic plate. The solid line is the beam, and the dashed line is the  $\langle 100 \rangle$  axis, which is perpendicular to the target surface.

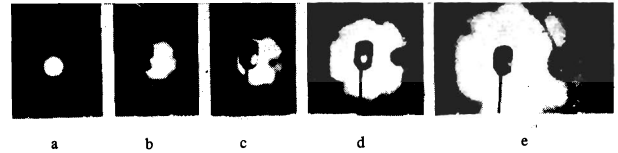


FIG. 4. Proton photographs: a— $E = 500 \text{ keV}$ ,  $\theta = 0.3^\circ$ ; b— $E = 500 \text{ keV}$ ,  $\theta = 0.8^\circ$ ; c— $E = 500 \text{ keV}$ ,  $\theta = 1.8^\circ$ ; d— $E = 500 \text{ keV}$ ,  $\theta = 2.8^\circ$ ; e— $E = 200 \text{ keV}$ ,  $\theta = 5.3^\circ$ .

In order to study the scattering at small angles, the target was mounted in a vacuum chamber on a goniometer head which permitted rotation in two mutually perpendicular planes with an accuracy of  $\pm 0.1^\circ$ . A proton beam of diameter  $0.3 \text{ mm}$  with an angular spread  $\Delta\theta \leq 0.05^\circ$  hit the target at an angle  $\theta$  to the  $\langle 100 \rangle$  axis (Fig. 3). The azimuthal orientation of the crystal was such that the ZOZ plane, which passes through the beam axis and the crystallographic  $\langle 100 \rangle$  axis, was close to the crystallographic (013) plane for all  $\theta$ , deviating from it by not more than  $10^\circ$ . Protons scattered at small angles were detected by a photographic plate placed at a distance of  $10 \text{ cm}$  from the target, perpendicular to the beam. A monitor counter was used to determine the exposure. Here the dependence of the intensity of particles recorded by the counter on target orientation was taken into account (see Fig. 2). The photographic plates were exposed until visible blackening appeared at several values of  $\theta$  and proton energies  $E$  of  $200$  and  $500 \text{ keV}$ .

The angular distribution of protons scattered in a thin target at small angles, as was expected, turned out to be sharply anisotropic; the drop in intensity in the range of angles of interest to us was as great as  $10^3$ . At the same time the photographic plate permits reliable detection of particles at intensities differing by not more than  $20$ – $50$  times. In order that the optical density nowhere exceed the linear portion of the density curve, the angular distributions were taken in parts, with different exposures. For this purpose, at the time of exposure of the peripheral portions, the central, more intense region of the distribution was blocked by a special screen (see Fig. 3) which is visible in the proton photographs of Fig. 4.

For a part of the plates to be used in the experiment, densitometry characteristics were obtained for proton energies of  $200$  and  $500 \text{ keV}$ , which turned out to be linear over the range  $0 < \log(1/S) < 2$ , where  $S$  is the optical density<sup>[5]</sup>. The proton photographs obtained during the course of the experiment were photometered, and scattered-proton angular distributions were plotted from the photometric data.

FIG. 5. Angular distribution: a—in the plane ZO<sub>X</sub> passing through the beam axis and the crystallographic (100) axis, and b—in the plane ZO<sub>Y</sub>. I is the intensity,  $\vartheta_x$  is the angle relative to the incident beam direction,  $\vartheta_m$  is the angle at which the maximum intensity of the reflected particle group is observed,  $\vartheta_y$  is the angle relative to the crystallographic (100) axis. Curve 1— $I(\vartheta_x)$ , 2— $I(-\vartheta_x)$ ,  $E = 500$  keV,  $\theta = 2.8^\circ$ .

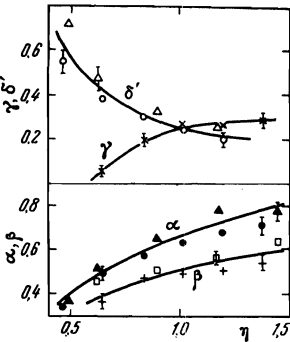
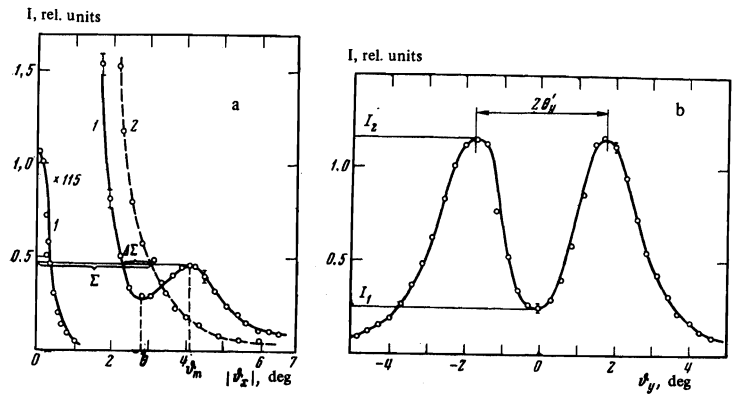


FIG. 6. Dependence of a number of parameters of the angular distributions on the angle of incidence  $\theta$  ( $\eta = \theta/\theta_b$ ):  $\circ$ — $\delta'$  for  $E = 500$  keV;  $\Delta$ — $\delta'$  for  $E = 200$  keV;  $\times$ — $\gamma$  for  $E = 500$  keV;  $\blacktriangle$ — $\beta = \theta_y'/\theta_b$  for  $E = 200$  keV;  $\bullet$ — $\beta$  for  $E = 500$  keV;  $\square$ — $\alpha = \theta_x'/\theta_b = (\vartheta_m - \theta)/\theta_b$ ,  $E = 200$  keV;  $+$ — $\alpha$  for  $E = 500$  keV.

Figure 4 shows some of the proton photographs obtained in the experiment. Our attention is caught by the absence of the characteristic stars with increased particle intensity which appear in channeling experiments in thicker crystals<sup>[6]</sup>. This is apparently due to the fact that channeling as such cannot develop completely during the time of motion of the particle in a thin sample. However, the shadows in Fig. 4 appear quite clearly. Even at a small angle  $\theta$ , plane shadows appear, and then, within increasing  $\theta$ , axial shadows. It can be seen from Fig. 4 that on rotation of the crystal about the beam the shadow pattern is shifted correspondingly, while the intensity maximum of the transmitted beam remains in place. This differs substantially from the case of a thick target, where the transmitted beam maximum is shifted.

The shape of the experimental angular distributions in the ZO<sub>X</sub> and ZO<sub>Y</sub> planes (Fig. 5) agrees for the most part with the qualitative ideas discussed above. In particular, a large drop is observed in the intensities of the peaks in the angular distributions in the ZO<sub>X</sub> plane.

Figure 6 provides the possibility of tracing the change in the angular-distribution parameters with change of incidence angle. The reflection angles  $\theta_y'$  and  $\theta_x'$  increase with increasing  $\theta$ , as should occur in scattering by an atomic string. For the maximal value  $\theta = 1.5 \theta_b$  used in the experiment, the values of  $\theta_x'$  and  $\theta_y'$  still do not reach their limiting value  $\theta' = \theta_b$ . The model arguments given above do not permit prediction of the rate of increase of the functions  $\theta_x'(\theta)$  and  $\theta_y'(\theta)$ . It must be kept in mind that for small angles  $\theta$ , even though  $\theta$  exceeds  $\theta_L$ , the shape of the shadow is strongly distorted by the sharply anisotropic angular distribution of the particles scat-

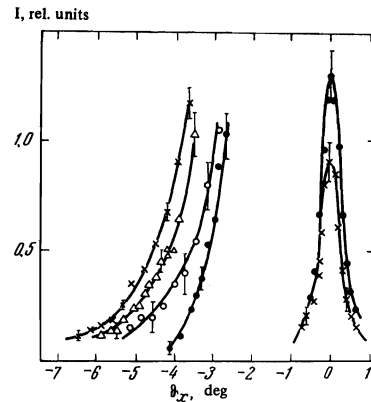


FIG. 7. Angular distributions of protons scattered in the plane ZO<sub>X</sub> for various values of  $\theta$  and  $E = 500$  keV. The intensity at all points of the angular distributions corresponds to the same number of particles incident on the target:  $\bullet$ — $\theta = 0$ ,  $\circ$ — $\theta = 1.3^\circ$ ,  $\Delta$ — $\theta = 1.8^\circ$ ,  $\times$ — $\theta \geq 2.8^\circ$ .

tered in the thin target at small angles. This distortion can lead to some decrease of  $\theta_x'$  and  $\theta_y'$  in comparison with the value  $\theta' = \theta_b$ . An estimate of the effect of the anisotropy of the angular distribution on the location of the shadow breastwork, made on the basis of a two-particle model, gives for the quantity  $\theta_b - \theta_x'$ , for example for  $\theta = 2.5 \theta_b$  and  $\sigma = 0.3 \theta_b$ , the value  $\theta_b - \theta_x' \approx 0.1 \theta_b$ . The values of  $\theta_x'$  obtained for energies of 200 and 500 keV and plotted in the graph of Fig. 6 in units of the angle  $\theta_b$  are grouped around a single curve. The values of  $\theta_y'$  behave in the same way. The relative intensity at the minimum of the angular distributions in the ZO<sub>Y</sub> plane decreases with increasing  $\theta$ , approaching a value  $\delta' = I_1/I_2 = \delta$  (see Fig. 2).

The angular distributions in the ZO<sub>X</sub> plane had very small angles relative to the beam directions  $0 \leq \vartheta_x \leq 0.5^\circ$  have a shape close to Gaussian (Fig. 7). For a variation of the angle of incidence from  $\theta = 0$  to  $\theta = 1.5 \theta_b$  the half-width of the distribution changes insignificantly. The intensity at the peak of the angular distribution in the same range of angles of incidence changes by a factor of 1.5. It is clear that the parameter values obtained for the angular distributions in this region of angles are determined to a significant degree by the angular resolution of the experiment. Figure 7 shows some of the angular distributions of protons scattered in the ZO<sub>X</sub> plane at negative angles relative to the beam direction. It is evident that these distributions are somewhat narrowed as the angle of incidence

$\theta$  decreases. This is due to the decrease in the yield of scattered particles whose trajectories lie far from the reflection cone. These particles appear mainly as the result of backward scattering at a large angle on intersection of the string by the incident protons. For  $\theta_x > 0$  the yield of singly scattered particles is suppressed in the region of the shadow, and therefore we can assume that the gap of width  $\Delta\Sigma$  between the dashed and solid curves in Fig. 5a somehow characterizes the fraction of particles which penetrate the string. The probability of intersecting the string evidently must decrease rapidly as the angle of incidence decreases, beginning with the value  $\theta \approx \theta_b$ . Accordingly, the curve  $\gamma(\eta)$  falls off quite steeply for  $\eta \leq 1$  ( $\gamma = \Delta\Sigma/\Sigma$ , Fig. 6). The experimental errors plotted in the curves of Figs. 5–7 are determined mainly by the errors in monitoring and in the photometric method of particle detection.

Thus, the regularities found in the experiment are in agreement with the qualitative ideas of interaction of protons with single strings or a small number of strings of atoms. The fact that multiple collisions are important here shows up in the existence of plane shadows, which are present in almost all the proton photographs of Fig. 4. Shadows corresponding to the low-index planes (100) and (110) are visible.

Study of the angular distributions of protons scattered in a thin single-crystal target permit a better understanding of some features of the passage of particles through thick crystals, which is accompanied by a large number of collisions with atomic strings. In fact, particles which have experienced a small number of collisions with strings in a thin target (Fig. 5) acquire an appreciable spread in angle relative to the crystallographic axis direction. For particles initially moving in the channeling mode ( $\theta < \theta_L$ ), this should lead to dechanneling. In the case in which the initial

angle exceeds  $\theta_b$ , which is characteristic for shadow formation, the shift in the intensity maximum of the reflected particles toward the axis ( $\eta < 1$ , Fig. 6) should play an important role. This facilitates the transition of particles to the channeling mode and the reduction of the depth of the shadow.

The authors are grateful to A. L. Afanas'ev, V. S. Kulikauskas, and G. P. Pokhil for assistance in carrying out the present work, and also to Yu. S. Korobochko, A. M. Markus, V. G. Sukharevskii, and A. I. Fedorenko for consultation and assistance in preparation of the targets.

<sup>1</sup>J. Lindhard, *Mat. Fys. Medd. Dan. Vid. Selsk.* **34**, No. 14, (1965).

<sup>2</sup>A. G. Kadmenskiĭ and A. F. Tulinov, *Tr. III Vsesoyuznogo soveshchaniya po fizike vzaimodeĭstviya zaryazhennykh chastits s monokristallami* (Proceedings, III All-union Conf. on the Physics of Interaction of Charged Particles with Single Crystals), Nuclear Physics Institute, Moscow State University, 1971.

<sup>3</sup>D. W. Pashley, *Phil. Mag.* **4**, 324 (1959).

<sup>4</sup>A. F. Tulinov, *Dissertation*, Moscow State University, 1967.

<sup>5</sup>A. G. Polandov, *Tr. III Vsesoyuznogo soveshchaniya po fizike vzaimodeĭstviya zaryazhennykh chastits s monokristallami* (Proceedings, III All-union Conf. on the Physics of Interaction of Charged Particles with Single Crystals), Nuclear Physics Institute, Moscow State University, 1971.

<sup>6</sup>G. Dearnaley, I. V. Mitchell, R. S. Nelson, B. W. Farmery, and M. W. Thompson, *Phil. Mag.* **18**, 985 (1968).